

On Bifurcations of Equilibria of Intrinsically Curved, Electrically Charged, Rod-like Structures that Model DNA Molecules in Solution

Yoav Y. Biton · Bernard D. Coleman · David Swigon

Received: 29 June 2006 / Accepted: 3 February 2007 /
Published online: 30 May 2007
© Springer Science + Business Media B.V. 2007

Abstract DNA molecules in the familiar Watson–Crick double helical B form can be treated as though they have rod-like structures obtained by stacking dominoes one on top of another with each rotated by approximately one-tenth of a full turn with respect to its immediate predecessor in the stack. These “dominoes” are called *base pairs*. A recently developed theory of sequence-dependent DNA elasticity (Coleman, Olson, & Swigon, *J. Chem. Phys.* 118:7127–7140, 2003) takes into account the observation that the step from one base pair to the next can be one of several distinct types, each having its own mechanical properties that depend on the nucleotide composition of the step. In the present paper, which is based on that theory, emphasis is placed on the fact that, as each base in a base pair is attached to the sugar-phosphate backbone chain of one of the two DNA strands that have come together to form the Watson–Crick structure, and each phosphate group in a backbone chain bears one electronic charge, two such charges are associated with each base pair, which implies that each base pair is subject to not only the elastic forces and moments exerted on it by its neighboring base pairs but also to long range electrostatic forces that, because they are only partially screened out by positively charged counter ions, can render the molecule’s equilibrium configurations sensitive to changes in the concentration c of salt in the medium. When these electrostatic forces are taken into account, the equations of mechanical equilibrium for a DNA molecule with $N+1$ base pairs are a system of μN non-linear equations, where μ , the number of kinematical variables describing the relative displacement and orientation of adjacent pairs is in general 6; it reduces to 3 when base-pair steps are assumed to be inextensible and non-shearable. As a consequence of the long-range

Y. Y. Biton · B. D. Coleman (✉)
Department of Mechanics & Materials Science, Rutgers University,
Piscataway, NJ 08854-8058, USA
e-mail: yoavbi@rci.rutgers.edu, bcoleman@jove.rutgers.edu

D. Swigon
Department of Mathematics, University of Pittsburgh, Pittsburgh, PA 15260, USA
e-mail: swigon@pitt.edu

electrostatic interactions of base pairs, the $\mu N \times \mu N$ Jacobian matrix of the equations of equilibrium is full. An efficient numerically stable computational scheme is here presented for solving those equations and determining the mechanical stability of the calculated equilibrium configurations. That scheme is employed to compute and analyze bifurcation diagrams in which c is the bifurcation parameter and to show that, for an intrinsically curved molecule, small changes in c can have a strong effect on stable equilibrium configurations. Cases are presented in which several stable configurations occur at a single value of c .

Keywords Sequence dependent DNA elasticity · Electrically charged rod-like structures · Bifurcation theory

Mathematics Subject Classifications (2000) 92-08 · 92D20 · 74K10 · 74B20 · 74G60 · 74G65

1 Introduction

For many purposes a molecule of duplex DNA can be treated as though it is a rod-like structure that in a nanoscale drawing looks roughly like a stack of dominos (called *base pairs*) with each rotated approximately 36° relative to the one below it in the stack. A base pair is formed by joining together two nearly planar complementary nucleotide bases each of which is attached to one of two sugar-phosphate chains. At the present time it appears reasonable to assume that the elastic energy Ψ of a DNA configuration¹ is the sum over n of the energy ψ^n of interaction of the n th and $(n+1)$ th base pairs and that ψ^n is given by a function of six numbers, called the *kinematical variables* (for the n th base pair step) that describe the orientation and displacement of the $(n+1)$ th base pair in the stack relative to the n th. The values of these variables in the stress-free state and the function giving ψ^n depend on which nucleotide bases are in the n th and $(n+1)$ th base pairs. Thus the genetic information in DNA determines not only the amino acid sequences of encoded proteins but also the intrinsic geometry and deformability of DNA at the level of base-pair steps.

A naturally discrete theory of DNA elasticity that is based on the assumption that $\Psi = \sum_n \psi^n$, with ψ^n given by a function of six kinematical variables [1, 2], because it takes into account the dependence of mechanical properties on nucleotide sequence, yields a model of DNA elasticity that is closer than the familiar continuum models to what we now know about the structure and deformability of DNA.

Important to the present discussion is the fact that because each base in a base pair is covalently bound to the sugar-phosphate backbone chain of one of the two DNA strands that form the Watson–Crick structure and each phosphate group bears one (negative) electronic charge, two such charges are associated with one base pair. The charges associated with two distinct base pairs exert on each other an electrostatic force of repulsion, the strength of which depends on the distance between them and the concentration c of salt in the aqueous solution of DNA. The dependence on c results from the fact that salt ions of positive charge form clouds around the negatively charged

¹We here use the term *configuration* as it is generally used in modern continuum mechanics and in the theory of rods and structures. However, in discussions of such topics as protein structure and the chemical physics of polymeric molecules, what we here call a “configuration” is often called a “conformation”.

sites on the DNA and in so doing partially screen out the electrostatic interaction of each site with others. As a consequence, an increase in c decreases the repulsion of nonadjacent base pairs and weakens the tendency of electrostatic forces to straighten DNA molecules. Despite this partial screening, even under physiological conditions a DNA molecule is subject to intramolecular electrostatic forces that under appropriate circumstances (e.g., when the molecule has intrinsic curvature) can cause equilibrium configurations to be sensitive to the concentration of salt in the medium. As a consequence, DNA is not what in contemporary continuum mechanics is called “a simple material”, “a higher gradient material”, or even a material with mechanical behavior that can be well approximated by the behavior of such materials.

In the present essay we present a theory of the equilibrium configurations of electrically charged and intrinsically curved rod-like structures that we believe serve as useful models of DNA molecules in aqueous solution. The theory goes beyond that of references [1] and [2] in that it renders explicit the nature and implications of electrostatic interactions between nonadjacent base pairs. Both here and in those papers, the variational equations of mechanical equilibrium for a DNA molecule with $N+1$ base pairs (bp) form a nonlinear system \mathcal{S} of μN equations for the μN unknown kinematical variables characterizing a configuration, where μ , the number of such variables at each base-pair step is, in general, 6 but reduces to 3 when two neighboring base pairs are (or are assumed to be) much stiffer for changes in their relative displacement than for changes in their relative orientation.

When, as in [1] and [2], the electrostatic forces are not rendered explicit, \mathcal{S} is a system of weakly coupled equations. Here, in marked contrast to those studies, because the force on a base pair depends on the position in space of all the other base pairs in the DNA molecule, the $\mu N \times \mu N$ Jacobian matrix for \mathcal{S} is full. The system \mathcal{S} here depends on the salt concentration c , and the influence of c on the geometry and stability of equilibrium configurations is a matter of importance.

The mathematical assumptions of our theory are stated in Section 2. In Section 3 we present an efficient procedure for solving the system \mathcal{S} and determining the stability of the resulting equilibrium configurations. Toward the end of the paper, in Section 4, we apply that procedure to an example of a 450 bp DNA molecule that can be thought of as having been formed by the end-to-end joining of three 150 bp DNA segments that are assumed to be homogeneous and to have uniform curvature such that in an intrinsic (stress-free) configuration each would have the shape of a circular ring. That example illustrates the strong influence that changes in the salt concentration c can have on the equilibrium configurations of intrinsically curved DNA and yields a bifurcation diagram with regions in which two very different, but yet both locally stable, equilibrium configurations occur at the same value of c . In order to focus our attention on the role of electrostatic forces in determining the properties of equilibrium configurations, for that example the DNA molecule was deliberately chosen to be non-shearable and homogeneous in its mechanical properties.

2 Basic Assumptions and Governing Equations

As in [1] and [2] base pairs are represented here by rectangular objects, and the energy of a DNA molecule with $N+1$ base pairs (and hence N base-pair steps) is determined when there is given, for $n = 1, \dots, N+1$, both the location \mathbf{x}^n of the center of the rectangle \mathcal{B}^n that represents the n th base pair and a right-handed orthonormal triad $\mathbf{d}_1^n, \mathbf{d}_2^n, \mathbf{d}_3^n$ that is

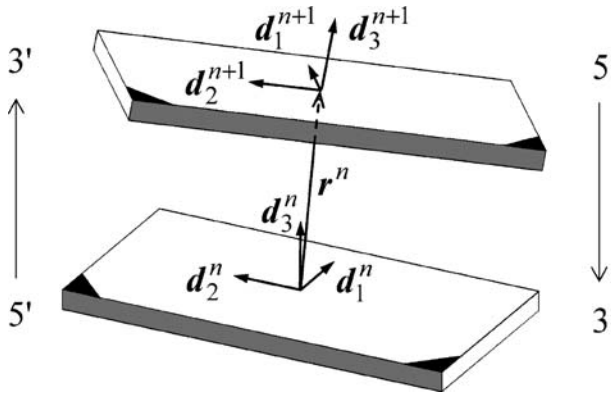


Fig. 1 Schematic drawing of the n th base-pair step showing the vectors r^n , d_i^n , and d_i^{n+1} . Each nucleotide base in the n th base pair lies mainly on one side of the plane spanned by d_1^n and d_3^n and is covalently bonded at its darkened corner to one of the two sugar phosphate chains. The direction of that oriented chain is indicated by a light-face arrow; the chain itself is not shown. The gray-shaded long edges are in the minor groove of the DNA

embedded in the base pair as shown in Fig. 1.² The polygonal curve \mathcal{C} composed of the N line segments that connect the spatial points x^1, x^2, \dots, x^{N+1} is called the *axial curve* of the molecule. The *elastic energy* Ψ of a configuration is taken to be the sum over n of the energy ψ^n of interaction of the n th and $(n+1)$ th base pairs, i.e.,

$$\Psi = \sum_{n=1}^N \psi^n, \tag{2.1}$$

where ψ^n , the elastic energy of the n th base-pair step, is given by a function of the relative orientation and displacement of the $(n+1)$ th base pair with respect to the n th, i.e., by a function of the components (with respect to the basis d_1^n, d_2^n, d_3^n) of the vectors d_j^{n+1} and $r^n = x^{n+1} - x^n$. The components $D_{ij}^n = d_i^n \cdot d_j^{n+1}$ of the vectors d_j^{n+1} form a 3×3 orthogonal matrix that is determined by three angles, $\theta_1^n, \theta_2^n, \theta_3^n$, called the *tilt*, *roll*, and *twist* (see Fig. 2). The displacement variables, $\rho_1^n, \rho_2^n, \rho_3^n$, called *shift*, *slide*, and *rise*, are related to the components $r_i^n = r^n \cdot d_i^n$ of r^n by a coordinate transformation of the type

$$\rho_i^n = \bar{\rho}_i(\theta_1^n, \theta_2^n, \theta_3^n, r_1^n, r_2^n, r_3^n), \tag{2.2}$$

which can be written in the form

$$\rho_i^n = \sum_{j=1}^3 \widehat{R}_{ji}(\theta_1^n, \theta_2^n, \theta_3^n) r_j^n. \tag{2.3}$$

²As seen in Fig. 1, the vectors d_i^n are defined so that d_3^n is perpendicular to \mathcal{B}^n with $d_3^n \cdot (x^{n+1} - x^n) > 0$; d_2^n is parallel to the long edges of \mathcal{B}^n and points toward the short edge containing the corner of \mathcal{B}^n that is covalently bonded to the sugar-phosphate chain for which n increases in the 5'-3' direction; $d_1^n = d_2^n \times d_3^n$ is parallel to the short edges of \mathcal{B}^n and points toward the major groove of the DNA. A detailed discussion is given in [3].

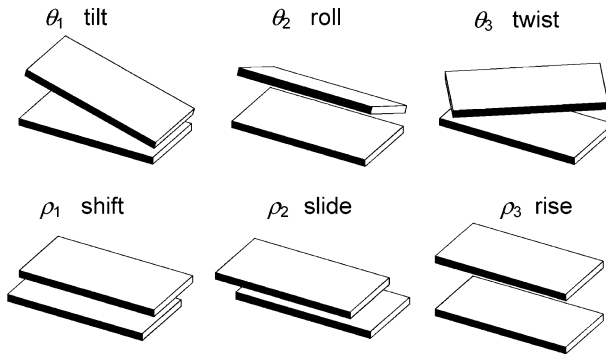


Fig. 2 Schematic representations of the kinematical variables that describe the relative orientation and displacement of consecutive base pairs: θ_1 and θ_2 are angles of rotation about two perpendicular lines that lie in the midplane between the base pairs; θ_3 is an angle of rotation about a line l perpendicular to the midplane; ρ_1 and ρ_2 are mutually perpendicular displacements in directions parallel to the midplane; and ρ_3 is a displacement along l . Each drawing illustrates one of the kinematical variables for the (artificial) case in which that variable has a positive value and the others (with the exception of ρ_3) are set equal to zero

The numbers $R_{ji}^n = \widehat{R}_{ji}(\theta_1^n, \theta_2^n, \theta_3^n)$ are the components of an orthogonal matrix, and the functions $\widehat{\rho}_i$ and \widehat{R}_{ji} appearing are independent of n . The elastic energy ψ^n of the n th base-pair step is thus given by a function $\widetilde{\psi}^n$ of six kinematical variables:

$$\psi^n = \widetilde{\psi}^n(\theta_1^n, \theta_2^n, \theta_3^n, \rho_1^n, \rho_2^n, \rho_3^n). \tag{2.4}$$

The function $\widetilde{\psi}^n$ in the constitutive equation (2.4) depends on the nucleotide composition of the n th and $(n+1)$ th base pairs. Unless one states otherwise, it is assumed that $\widetilde{\psi}^n$, as a function of $(\theta_1^n, \theta_2^n, \theta_3^n, \rho_1^n, \rho_2^n, \rho_3^n)$ alone, is independent of the nucleotide composition of other base pairs, e.g., the $(n-1)$ th and $(n+2)$ th, from which it follows that a base-pair step can be one of ten different types. However, our theory remains valid in more general cases in which the function $\widetilde{\psi}^n$ is assumed to be influenced by the composition of such other base pairs.

The kinematical variables θ_i^n and ρ_i^n were introduced by Zhurkin et al. [4] and El Hassan and Calladine [5]. They are defined with precision in [5]. Properties of functions, such as $\widehat{\rho}_i$, that relate ρ_i^n and θ_i^n to r_i^n and D_{ij}^n are discussed in detail in [1, 2, 5], and the Appendix in this paper. The variables θ_i^n and ρ_i^n are such that, for each fixed configuration of the DNA molecule, a change in the choice of the direction of increasing n leaves $\theta_2, \theta_3, \rho_2, \rho_3$ invariant but changes the sign of θ_1 and ρ_1 .³

We here consider a DNA molecule in an aqueous solution with a concentration c of a monovalent salt (e.g., NaCl). We assume that no external forces or moments act on a base pair other than those that result from the long range electrostatic interaction of negatively charged phosphates in the same polymeric molecule. We further assume, as an approximation, that the two negative charges associated with each base pair are located at the barycenter of that base pair which implies that the electrostatic energy of a configuration has the form,

$$\Phi = \frac{1}{2} \sum_{n=1}^{N+1} \varphi^n, \quad \varphi^n = \widetilde{\varphi}^n(\mathbf{x}^1, \dots, \mathbf{x}^{N+1}), \tag{2.5}$$

³General implications of this remark for the functions $\widetilde{\psi}^n$ are given in [1]. See also the remark made below after equation (2.21).

(in which φ^n is the electrostatic energy associated with the n th base pair) and hence that base pairs do not sustain moments of electrostatic origin. In the present theory we employ Manning’s theory of charge condensation, which, as discussed in the paragraph containing equation (2.23), is in accord with equation (2.5).

A configuration of the DNA molecule is said to be in *equilibrium* if the first variation of the total energy,

$$U = \Psi + \Phi, \tag{2.6}$$

vanishes for all variations that are compatible with the constraints imposed on the molecule.

Equation (2.5) and the theory developed in reference [1] here yield equations of equilibrium that can be written in the form,

$$\mathbf{f}^n - \mathbf{f}^{n-1} + \mathbf{g}^n = \mathbf{0}, \quad \mathbf{m}^n - \mathbf{m}^{n-1} + \mathbf{r}^n \times \mathbf{f}^n = \mathbf{0}, \quad n = 1, 2, \dots, N. \tag{2.7}$$

For $n=1,2,\dots, N$, \mathbf{f}^n and \mathbf{m}^n are the (non-electrostatic) force and moment that the $(n+1)$ th base pair exerts on the n th. The vectors $-\mathbf{f}^0$ and $-\mathbf{m}^0$ equal the force and moment that the external world exerts on the base pair for which $n=1$; when the DNA molecule is assumed free of such external forces and moments,

$$\mathbf{f}^0 = \mathbf{0}, \quad \mathbf{m}^0 = \mathbf{0}, \quad \mathbf{g}^{N+1} - \mathbf{f}^N = \mathbf{0}, \quad \mathbf{m}^N = \mathbf{0}. \tag{2.8}$$

In (2.7) and (2.8), \mathbf{g}^n equals the total electrostatic force exerted on the n th base pair by other base pairs in the same molecule and is given by the equation

$$\mathbf{g}^n = \sum_{m \neq n} \mathbf{G}^{mn} = - \frac{\partial \Phi}{\partial \mathbf{x}^n}. \tag{2.9}$$

Here $\mathbf{G}^{mn} = -\mathbf{G}^{nm}$ is the electrostatic force (of repulsion) that the m th base pair exerts on the n th; that force is directed along the line connecting the barycenters of the two base pairs. Using equation (2.9) one can show that the first two of the equations (2.8) together with the equations of equilibrium (2.7) imply the third and the fourth of the equations (2.8). In [1] it is shown that, for $n=1,2,\dots, N$, the components f_i^n and m_i^n of \mathbf{f}^n and \mathbf{m}^n with respect to the local basis $\mathbf{d}_1^n, \mathbf{d}_2^n, \mathbf{d}_3^n$ are

$$f_i^n = \sum_{j=1}^3 \frac{\partial \tilde{\psi}^n}{\partial \rho_j^n} \frac{\partial \tilde{\rho}_j}{\partial r_i^n}, \quad f_i^n = \mathbf{f}^n \cdot \mathbf{d}_i^n, \tag{2.10}$$

$$m_i^n = \sum_{j=1}^3 \Gamma_{ij}^n \left[\frac{\partial \tilde{\psi}^n}{\partial \theta_j^n} + \sum_{k=1}^3 \frac{\partial \tilde{\psi}^n}{\partial \rho_k^n} \frac{\partial \tilde{\rho}_k}{\partial \theta_j^n} \right], \quad m_i^n = \mathbf{m}^n \cdot \mathbf{d}_i^n, \tag{2.11}$$

where $\Gamma_{ij}^n = \hat{\Gamma}_{ij}(\theta_1^n, \theta_2^n, \theta_3^n)$ with $\hat{\Gamma}_{ij}$ a function independent of n whose form is known.⁴

⁴See equations (A.1–A.5), (2.12–2.15) of [1], or the Appendix to this paper.

The equations (2.7), when taken together with (2.8–2.11), form a system of $6N$ equations for the $6N$ scalar variables $\theta_1^n, \theta_2^n, \theta_3^n, \rho_1^n, \rho_2^n, \rho_3^n, n=1,2,\dots, N$. In the remainder of this paper we emphasize the limiting case in which the DNA molecule is stiff with respect to (i.e., strongly resistant to changes in) the kinematical quantities $\rho_1^n, \rho_2^n, \rho_3^n$ that characterize shift, slide, and rise. That limit is one in which the displacement parameters $\rho_1^n, \rho_2^n, \rho_3^n$ are preassigned constants. In the limit, \mathbf{f}^n , like the pressure p in an incompressible fluid, is no longer given by a local constitutive relation such as (2.10), but instead is determined by a balance law and boundary conditions. Here the appropriate balance law is the first equation of (2.7); the appropriate boundary conditions (here called *end conditions*) are the first and third equations of (2.8); these relations yield the expression,

$$\mathbf{f}^n = -\sum_{m=1}^n \mathbf{g}^m, \tag{2.12}$$

that, by (2.9) and (2.5), relates \mathbf{f}^n to the axial curve \mathcal{C} and hence to the vector

$$\Theta = (\theta_1^1, \theta_2^1, \theta_3^1, \theta_1^2, \dots, \theta_3^N) \tag{2.13}$$

in \mathbb{R}^{3N} . In the same limit, the term $(\partial\tilde{\psi}^n/\partial\rho_k^n)(\partial\tilde{\rho}_k/\partial\theta_j^n)$ in (2.11) loses meaning, and we have

$$m_i^n = \sum_{j=1}^3 \Gamma_{ij}^n \left[\frac{\partial\tilde{\psi}^n}{\partial\theta_j^n} - \sum_{k=1}^3 \sum_{l=1}^3 f_l^n \frac{\partial\hat{R}_{lk}}{\partial\theta_j^n} \rho_k^n \right]. \tag{2.14}$$

Here, as in (2.10) and (2.11), $f_i^n = \mathbf{f}^n \cdot \mathbf{d}_i^n$ and $m_i^n = \mathbf{m}^n \cdot \mathbf{d}_i^n$. When, as in the present case, the numbers $\rho_1^1, \rho_2^1, \rho_3^1, \rho_1^2, \dots, \rho_3^N$ are preassigned, it follows from the relations

$$r_i^n = \mathbf{r}^n \cdot \mathbf{d}_i^n, \quad \mathbf{x}^n = \mathbf{x}^1 + \sum_{p=1}^{n-1} \mathbf{r}^p, \tag{2.15}$$

the equation (2.3), and expressions given in the Appendix for the dependence of $D_{ij}^n = \mathbf{d}_i^n \cdot \mathbf{d}_j^{n+1}$ on $\theta_1^n, \theta_2^n, \theta_3^n$ that, if Θ is known, then, to within an arbitrary rigid body rotation and translation, the vectors $\mathbf{d}_1^1, \mathbf{d}_2^1, \mathbf{d}_3^1, \mathbf{d}_1^2, \dots, \mathbf{d}_3^{N+1}$ and the points $\mathbf{x}^1, \mathbf{x}^2, \dots, \mathbf{x}^{N+1}$ are also known, and hence we may refer to Θ as the *configuration* of the molecule.

Let us now concentrate our attention on *equilibrium configurations*, i.e., on solutions $(\theta_1^1, \theta_2^1, \theta_3^1, \theta_1^2, \dots, \theta_3^N)$ of the equations (2.7) and (2.8) in which $\mathbf{g}^n, \mathbf{f}^n$, and \mathbf{m}^n are given by (2.9), (2.12), and (2.14). An equilibrium configuration of a molecule obeying these hypotheses will here be called *stable* if the $3N \times 3N$ square matrix \mathbf{A} with the components,

$$A_{(i,n)(j,m)} = \frac{\partial^2}{\partial\theta_i^n \partial\theta_j^m} U(\theta_1^1, \theta_2^1, \theta_3^1, \theta_1^2, \dots, \theta_3^N), \quad i, j = 1, 2, 3, \quad n, m = 1, \dots, N, \tag{2.16}$$

is positive definite, i.e., if the second variation of the total energy,

$$\delta^2 U = \sum_{\substack{i=1,2,3 \\ n=1,\dots,N}} \sum_{\substack{j=1,2,3 \\ m=1,\dots,N}} A_{(i,n)(j,m)} \delta\theta_i^n \delta\theta_j^m, \tag{2.17}$$

is (strictly) positive for every non-zero variation

$$\delta\Theta = (\delta\theta_1^1, \delta\theta_2^1, \delta\theta_3^1, \delta\theta_1^2, \dots, \delta\theta_3^N) \tag{2.18}$$

of configuration. We are particularly interested in the way the shape and stability of equilibrium configurations depend on the salt concentration c .

We pause a moment to comment on our proposed criterion for stability. In applications of the present theory, equilibrium configurations of curved DNA molecules that are stable in the classical sense, but yet have symmetries implying the existence of variations with neutral directions, are rare. When they do occur, their presence is expected to be detectable so that such (neutral) variations are excluded when applying our criterion.

When $\rho_1^1, \rho_2^1, \rho_3^1, \rho_1^2, \dots, \rho_3^N$ are preassigned constants, the elastic energy associated with the n th base-pair step is given by a function $\widehat{\psi}^n$ of the three kinematical variables $\theta_1^n, \theta_2^n, \theta_3^n$:

$$\psi^n = \widehat{\psi}^n(\theta_1^n, \theta_2^n, \theta_3^n). \tag{2.19}$$

For the calculations to be reported here we make the additional assumption that this function is a quadratic form in the *excess tilt* $\Delta\theta_1^n$, the *excess roll* $\Delta\theta_2^n$, and the *excess twist* $\Delta\theta_3^n$, which quantities are defined so that

$$\theta_i^n = {}_o\theta_i^n + \Delta\theta_i^n, \tag{2.20}$$

where the ${}_o\theta_i^n$ are intrinsic values, i.e., values appropriate to a stress-free state of the n th base pair step. Thus

$$\psi^n = \frac{1}{2} \sum_{i=1}^3 \sum_{j=1}^3 F_{ij}^n \Delta\theta_i^n \Delta\theta_j^n, \tag{2.21}$$

where the moduli $F_{ij}^n = F_{ji}^n$ like the intrinsic parameters ${}_o\theta_i^n$ are constants that depend on the nucleotide composition of the n th and $(n+1)$ th base pairs. (Here, as is common practice, it is assumed that the elastic moduli and intrinsic parameters are independent of the nucleotide composition of other base pairs, but our general theory and computational schemes do not require such an assumption.)

One may think of F_{11}^n and F_{22}^n as the (local) coefficients of rigidity for bending and of F_{33}^n as the corresponding coefficient for twisting. Quadratic energy functions of the form (2.21) are approximations useful for small values of $\Delta\theta_i^n$.

The observation made at the beginning of this section to the effect that a change in the choice of the direction of increasing n leaves θ_2 and θ_3 invariant but changes the sign of θ_1 here places no *á priori* restriction on the modulus F_{23}^n coupling roll to twist but does imply that the moduli that couple tilt to roll and tilt to twist obey the relations

$$F_{12}^n = -\overleftarrow{F}_{12}^{N-n+1}, \quad F_{13}^n = -\overleftarrow{F}_{13}^{N-n+1}, \tag{2.22}$$

where $\overleftarrow{F}_{12}^{N-n+1}$ and $\overleftarrow{F}_{13}^{N-n+1}$ are moduli associated with a base-pair step that is complementary to the n th step. (For example, if a step has on one strand the sequence AG (or AT), then for its complementary step the corresponding sequence is CT (or AT)). It follows that if the n th step is self-complementary, i.e., has the sequence AT, TA, GC, or CG, then (as discussed in [1]) $F_{12}^n = 0, F_{13}^n = 0$.

For calculations of electrostatic interactions we here employ a form of Manning's theory of charge condensation [6] and obtain the following expression for the energy resulting

from the electrostatic interaction between the charge associated with the n th base pair and the charges associated with other base pairs:⁵

$$\varphi^n = Q \sum_{\substack{m \neq n \\ m \neq n \pm 1}} \frac{e^{-\kappa x^{nm}}}{x^{nm}}, \quad x^{nm} = |\mathbf{x}^n - \mathbf{x}^m|. \tag{2.23}$$

When measured in units of \AA^{-1} , the Debye screening parameter κ is given by the formula

$$\kappa = 0.329\sqrt{c}, \tag{2.24}$$

where c is the concentration of (monovalent) salt in moles per liter. For the constant Q we have

$$Q = q^2 / 4\pi\epsilon_0\epsilon_w, \tag{2.25}$$

with ϵ_0 the permittivity of free space and ϵ_w the dielectric constant of water, and, in accord with Manning’s theory [6, 8], q is set equal to 24% of the charge of the two phosphate groups associated with each base pair, i.e., $q = 2 \times 0.24e^-$, where e^- is the charge of an electron. For each n the summation in (2.23) is taken over all m from 1 to $N+1$ that correspond to base pairs that are not adjacent to, or the same as, the n th base pair. Nearest neighbors are omitted from that summation because we take the position that the local elastic energy functions $\tilde{\psi}^{n-1}$ and $\tilde{\psi}^n$ account for all interactions (including those of electrostatic origin) between the n th base pair and the two that are adjacent to it. When we insert (2.23) into (2.5) and make use of (2.9), we obtain for the vector \mathbf{g}^n the relation

$$\mathbf{g}^n = Q \sum_{\substack{m \neq n \\ m \neq n \pm 1}} \frac{e^{-\kappa x^{nm}}}{x^{nm}} \left(\frac{1}{x^{nm}} + \kappa \right) \frac{\mathbf{x}^n - \mathbf{x}^m}{x^{nm}}. \tag{2.26}$$

Because knowledge of the $3N$ -dimensional vector Θ determines the vectors \mathbf{x}^n (see the sentence containing equation (2.15)), this last equation tells us that \mathbf{g}^n is given by a function of Θ (which, albeit complicated, can be rendered explicit), and, by (2.12) and (2.14), so also are the vectors \mathbf{f}^n and \mathbf{m}^n .

When we write equation (2.12) we are assuming that the force vectors \mathbf{f}^n obey the first of the equilibrium equations (2.7) and the end condition $\mathbf{f}^0 = \mathbf{0}$, which relations then yield the third of the equations (2.8). We obtain an equilibrium configuration when we find a $3N$ -dimensional vector Θ that obeys the second of the equations (2.7) with \mathbf{m}^n as in (2.14) and \mathbf{f}^n as in (2.12).

To cast the second of the equations (2.7) into a form convenient for calculations, let us now write $\bar{m}_i^n, \bar{f}_i^n, \bar{r}_i^n$ for the components of $\mathbf{m}^n, \mathbf{f}^n, \mathbf{r}^n$ with respect to the basis $\mathbf{d}_1^1, \mathbf{d}_2^1, \mathbf{d}_3^1$. These components are related to the components of the same vectors with respect to the basis $\mathbf{d}_1^n, \mathbf{d}_2^n, \mathbf{d}_3^n$ through equations of the form,

$$\bar{m}_i^n = \mathbf{d}_i^1 \cdot \mathbf{m}^n = \sum_{j=1}^3 \left(\mathbf{d}_i^1 \cdot \mathbf{d}_j^n \right) m_j^n, \tag{2.27}$$

⁵See also the discussion of Westcott et al. [7].

etc., and hence depend on Θ . In this notation, the second of the equations (2.7) becomes

$$\Omega(\Theta) = \mathbf{0}, \quad \text{i.e., } \omega_i^n(\Theta) = 0, \quad i = 1, 2, 3, \quad n = 1, 2, \dots, N, \quad (2.28)$$

where

$$\Omega = (\omega_1^1, \omega_2^1, \omega_3^1, \omega_1^2, \dots, \omega_3^N), \quad (2.29)$$

with

$$\omega_i^n = \bar{m}_i^n - \bar{m}_i^{n-1} + \sum_{j=1}^3 \sum_{k=1}^3 \bar{r}_j^n \bar{r}_k^n e_{ijk}, \quad (2.30)$$

and e_{ijk} is the permutation symbol. We are particularly interested in bifurcation diagrams for the dependence of the solutions of equation (2.28) on the salt concentration c . The procedure by which we numerically solve the $3N$ equations (2.28) and determine the stability of the equilibrium configurations so obtained is described below.

Remark When we wrote the equation (2.5) which, because we employ Manning’s charge condensation theory, yields the equations (2.23–2.26), we made an approximation that will be noticed by readers familiar with current ideas about DNA structure and base-pair level models of DNA elasticity. We assumed “that the two negative charges associated with each base pair are located at the barycenter of that base pair.” In fact, those negative charges belong to the phosphate groups of two sugar phosphate chains that are at the surface of the DNA double helix and not at its center. However, Manning’s theory gives us reason for expecting that the condensed counter ions (which, in the case of DNA in an aqueous solution of monovalent salt, neutralize 76% of the charged phosphate groups) are not actually bound to the DNA macromolecule, i.e., are not localized at definite sites on that molecule, but are instead free to move in and out (and also along the axis) of a tube that has a diameter that depends on c but exceeds the 20 Å steric diameter of the macromolecule. When one accepts the idea that the net effective charge of the DNA macromolecule is not to be thought of as arising from charges at preassigned points but rather as the result of rapid fluctuations in a region interior to a tube of specified radius, it appears reasonable to suppose that the assumption stated in quotes above does not introduce serious errors.

3 Computational Procedure

To solve the system of equations (2.28) when there is available a configuration $*\Theta$ that is close to an equilibrium configuration Θ for the salt concentration c (for example, when one already has found an equilibrium configuration for a salt concentration $*c$ close to c), we put $\widehat{\Delta}\Theta = \Theta - *\Theta$, $\|\widehat{\Delta}\Theta\| = \max_{i,n} |\theta_i^n - *\theta_i^n|$ and write⁶

$$\mathbf{0} = \Omega(\Theta) = \Omega(*\Theta + \widehat{\Delta}\Theta) = \Omega(*\Theta) + \nabla\Omega(*\Theta) [\widehat{\Delta}\Theta] + O\left(\|\widehat{\Delta}\Theta\|^2\right), \quad (3.1)$$

⁶We here use the symbol $\widehat{\Delta}$ in place of Δ so that the components of $\widehat{\Delta}\Theta$ be distinguished from the quantities $\Delta\theta_i^n$ in equations (2.20) and (2.21).

where $\nabla\Omega(\ast\Theta) \left[\widehat{\Delta\Theta} \right]$ is linear in $\widehat{\Delta\Theta}$, i.e., $\nabla\Omega(\ast\Theta)$ is the gradient of the function $\Omega(\cdot)$ evaluated at the configuration $\ast\Theta$. This gradient is characterized by a $3N \times 3N$ square (but not symmetric) matrix \mathbf{B} with the components

$$B_{(i,n)(j,m)}(\ast\Theta) = \frac{\partial \omega_i^n}{\partial \theta_j^m}(\ast\Theta). \tag{3.2}$$

On omitting the terms $O\left(\|\widehat{\Delta\Theta}\|^2\right)$ one obtains the following system of $3N$ linear equations for the $3N$ components $\theta_i^n - \ast\theta_i^n$ of $\widehat{\Delta\Theta}$:

$$\omega_i^n(\ast\Theta) + \sum_{\substack{j=1,2,3 \\ m=1,\dots,N}} B_{(i,n)(j,m)}(\ast\Theta) \left(\theta_j^m - \ast\theta_j^m \right) = 0. \tag{3.3}$$

Although the matrix \mathbf{B} is full and has entries that depend on the θ_j^m -derivatives of the components $\overline{g}_i^n, \overline{f}_i^n$, and \overline{m}_i^n of $\mathbf{g}^n, \mathbf{f}^n$, and \mathbf{m}^n , we have been able to write a computer code that collects the large number of algebraic terms in each functional component of $\Omega(\cdot)$ and yields an analytical expression for each entry in \mathbf{B} as a function of the (known) components of $\ast\Theta$.⁷ Thus we avoid the need to employ numerical approximations for \mathbf{B} , and we obtain a stable and efficient code for solving the linear system (3.3) as one step in a Newton–Raphson iterative procedure that yields solutions of the nonlinear system (2.28) to within machine accuracy.

Once we have in hand a procedure for calculating equilibrium configurations, we can turn to the matter of determining whether such a configuration is (locally) stable in the sense that for it the matrix $\mathbf{A}=\mathbf{A}(\Theta)$ of equations (2.16) and (2.17) is positive definite. Because the equations (2.7) and (2.8) are equivalent to the statement that the first variation δU of U vanishes for each variation in the vectors $\mathbf{d}_i^n, i=1,2,3, n=1, \dots, N+1$, there is a useful algebraic relation between \mathbf{A} and the matrix \mathbf{B} characterizing the linearization $\nabla\Omega(\cdot)$ of the function $\Omega(\cdot)$ of equations (2.28–2.30) that follows from the following formula [1] expressing variations $\delta\theta_i^n$ in the numbers θ_i^n in terms of variations in the vectors \mathbf{d}_i^n :

$$\delta\theta_i^n = \sum_{j=1}^3 \Gamma_{ji}^n \mathbf{d}_j^n \cdot (\boldsymbol{\gamma}^{n+1} - \boldsymbol{\gamma}^n). \tag{3.4}$$

Here $\boldsymbol{\gamma}^n$ is the vector in the usual representation of the skew linear transformation, $\mathbf{d}_j^n \mapsto \delta\mathbf{d}_j^n$, as an outer product, i.e.,

$$\delta\mathbf{d}_j^m = \boldsymbol{\gamma}^m \times \mathbf{d}_j^m, \quad \text{for } j = 1, 2, 3, \tag{3.5}$$

and Γ_{ji}^n is as in (2.11). (More details are given in the Appendix.). If we put $\overline{\boldsymbol{\gamma}}_i^n = \boldsymbol{\gamma}^n \cdot \mathbf{d}_i^n$, we have

$$\delta U = - \sum_{\substack{i=1,2,3 \\ n=1,\dots,N+1}} \omega_i^n(\Theta) \overline{\boldsymbol{\gamma}}_i^n, \tag{3.6}$$

where $\omega_i^{N+1} = \overline{m}_i^N$. Equation (3.6) is equivalent to equation (3.20) of [1] and when combined with equations (2.28) and (2.30) yields

$$\delta^2 U = - \sum_{\substack{j=1,2,3 \\ m=1,\dots,N}} \sum_{\substack{i=1,2,3 \\ n=1,\dots,N+1}} \frac{\partial \omega_i^n}{\partial \theta_j^m}(\Theta) \delta\theta_j^m \overline{\boldsymbol{\gamma}}_i^n. \tag{3.7}$$

⁷In view of (2.24), (2.26), (2.12), and (2.14), those expressions contain c as a parameter.

By (3.2), we have, for $i, j=1,2,3$,

$$\frac{\partial \omega_i^n}{\partial \theta_j^m}(\Theta) = B_{(i,n)(j,m)}(\Theta) \quad \text{for } n, m = 1, \dots, N, \tag{3.8a}$$

$$\frac{\partial \omega_i^{N+1}}{\partial \theta_j^m}(\Theta) = \frac{\partial \bar{m}_i^N}{\partial \theta_j^m}(\Theta), \tag{3.8b}$$

and, by (2.17),

$$\partial \omega_i^p / \partial \theta_j^m = - \sum_{\substack{k=1,2,3 \\ n=1,\dots,N}} A_{(k,n)(j,m)} T_{(k,n)(i,p)}, \quad \text{for } p = 1, 2, \dots, N + 1. \tag{3.9}$$

Moreover, equation (3.7) can be written in the form

$$\delta^2 U = - \sum_{\substack{j=1,2,3 \\ m=1,\dots,N+1}} \sum_{\substack{i=1,2,3 \\ n=1,\dots,N+1}} S_{(i,n)(j,m)} \bar{\gamma}_i^n \bar{\gamma}_j^m, \tag{3.10}$$

where the numbers $S_{(i,n)(j,m)} = S_{(i,n)(j,m)}(\Theta)$ are the components of a $(3N + 3) \times (3N + 3)$ symmetric matrix **S** and obey the relation

$$S_{(i,n)(j,m)} = \sum_{\substack{k=1,2,3 \\ p=1,\dots,N}} \frac{\partial \omega_i^n}{\partial \theta_k^p} T_{(k,p)(j,m)}. \tag{3.11}$$

The numbers $T_{(k,p)(j,m)}$ in (3.11) and (3.9) are the components of the $3N \times (3N + 3)$ matrix **T** determining the linear transformation $\mathbb{R}^{3N+3} \rightarrow \mathbb{R}^{3N}$ that takes the vector $\mathbf{Y} = (\bar{\gamma}_1^1, \bar{\gamma}_2^1, \bar{\gamma}_3^1, \bar{\gamma}_1^2, \dots, \bar{\gamma}_3^{N+1})$ into the vector $\delta \Theta = (\delta \theta_1^1, \delta \theta_2^1, \delta \theta_3^1, \delta \theta_1^2, \dots, \delta \theta_3^N)$; i.e.,

$$\delta \Theta = \mathbf{T} \mathbf{Y}. \tag{3.12}$$

Equation (3.4) tells us that if one lets Γ^n , \mathbf{Q}^n , and \mathbf{O} be the 3×3 matrices with the components $\Gamma_{ij}^n = \widehat{\Gamma}_{ij}(\theta_1^n, \theta_2^n, \theta_3^n)$, $\mathbf{Q}_{ij}^n = \mathbf{d}_i^n \cdot \mathbf{d}_j^n$, and $O_{ij} = 0$, then **T** becomes the following $N \times (N + 1)$ matrix with entries that are 3×3 matrices:

$$\mathbf{T} = \begin{bmatrix} -\Gamma^{1T} \mathbf{Q}^1 & \Gamma^{1T} \mathbf{Q}^1 & \mathbf{O} & \mathbf{O} & \dots & \mathbf{O} \\ \mathbf{O} & -\Gamma^{2T} \mathbf{Q}^2 & \Gamma^{2T} \mathbf{Q}^2 & \mathbf{O} & \dots & \mathbf{O} \\ \mathbf{O} & \mathbf{O} & \ddots & \ddots & \ddots & \mathbf{O} \\ \vdots & \vdots & & & & \vdots \\ \mathbf{O} & \mathbf{O} & \mathbf{O} & \dots & -\Gamma^{NT} \mathbf{Q}^N & \Gamma^{NT} \mathbf{Q}^N \end{bmatrix}. \tag{3.13}$$

Here Γ^{nT} is the transpose of Γ^n . As the evaluation of the sparse matrix **T** is not a computationally expensive matter, it follows from (3.8a) and (3.8b) that once one has calculated the matrix **B**, which is given by (3.2) and characterizes the linearization $\nabla \Omega(\Theta)[\cdot]$ of the function $\Omega(\cdot)$ in the equation of equilibrium (2.28), one may employ (3.11) to calculate at small expense the symmetric matrix **S**.

Of course, the $3N \times 3N$ matrix **A** is positive definite if and only if all its proper numbers are (strictly) positive. The matrices **A** and **S** differ in the following important ways:

Whereas \mathbf{A} characterizes the second variation of the energy U with respect to variations $\delta\Theta$ in the vector Θ in \mathbb{R}^{3N} , which, because it describes (for each n) the orientation of the $(n+1)$ th base pair relative to the n th base pair, is invariant under rigid body motions of the DNA molecule, the $(3N + 3) \times (3N + 3)$ matrix \mathbf{S} characterizes the second variation of U with respect to variations in the $N+1$ triads $(\mathbf{d}_1^n, \mathbf{d}_2^n, \mathbf{d}_3^n)$ which are *not* invariant under rigid body motions of the molecule. In a configurational perturbation that is no more than a rigid body rotation, the vector \mathbf{Y} does not vanish, although the vector $\delta\Theta$ does. For the matrix \mathbf{A} to be positive definite it is necessary and sufficient that exactly 3 proper numbers of \mathbf{S} be zero and all the other proper numbers of \mathbf{S} be positive. Thus, *when the $3N+3$ proper numbers of \mathbf{S} are placed in a sequence $(0, 0, 0, \lambda_1, \lambda_2, \dots, \lambda_{3N})$ with $\lambda_1 \leq \lambda_2 \leq \dots \leq \lambda_{3N}$, the equilibrium configuration under consideration is stable if and only if λ_1 is greater than zero.*

In our study of the dependence of equilibrium configurations on salt concentration c , we calculate and present bifurcation diagrams in which c is the bifurcation parameter and λ_1 the ordinate. In such a diagram, an equilibrium configuration is stable when it corresponds to a point above the abscissa.

We caution the reader that our stability criterion that all the proper numbers of \mathbf{A} , or, equivalently, that all but 3 of the proper numbers of \mathbf{S} , be positive, is correct only in cases such as the present in which the DNA molecule is free of external loads and kinematical constraints and hence (2.8) holds. When the molecule is constrained so that \mathbf{Y} has values only in a (proper) subspace of \mathbb{R}^{3N+3} there will be an appropriate matrix other than \mathbf{S} that furnishes a necessary and sufficient spectral criterion for stability.

4 An Example Illustrating Strong Dependence of Equilibrium Configurations on Salt Concentration

A DNA molecule with an axial curve that is not a closed curve will here be called *open*. We conclude this essay with a presentation of computational results for an open molecule with 450 base pairs (i.e., with $N=449$). We assume that the molecule is free of external forces and moments and hence obeys (2.8). As we take the parameters $\rho_i^n, i=1,2,3$ and $n=1,\dots,N$, to be preassigned constants, we continue to employ the constitutive equation (2.21) for ψ^n . In the present case the equations of equilibrium (2.28–2.30), with \mathbf{f}^n and \mathbf{m}^n as in (2.12) and (2.14), yield a system \mathcal{S} of 1,347 equations. Our computational procedure is described in Section 3.

So as to have an elementary example, we employ constitutive relations that have transverse symmetry in the sense that: (1) for each n the shift and slide, ρ_1^n and ρ_2^n , are both zero and the rise ρ_3^n has the standard value of 3.4 Å; (2) the moduli F_{11}^n for tilt and F_{22}^n for roll in equation (2.21) are equal, and there is no coupling between tilt, roll, and twist:

$$F_{11}^n = F_{22}^n = \text{constant}, \quad F_{12}^n = F_{13}^n = F_{23}^n = 0. \tag{4.1}$$

In the present case we put: $F_{33}^n/F_{11}^n = 1.05$ and $F_{11}^n = F_{22}^n = 0.0427 \text{ kT/deg}^2$.

We here make assumptions about the parameters ${}_o\theta_i^n$ that are appropriate to a molecule formed by ligating, end to end, three DNA segments, each containing 150 base pairs and each having an intrinsic configuration in which it is circular in the sense that its axial curve is a perfect polygon of 150 sides. One way to obtain a model for such a molecule is to assume that it is homogeneous with, for each n , no intrinsic tilt, an intrinsic roll equal to $2\pi/150$ (i.e., 2.4°) and no intrinsic twist:

$${}_o\theta_1^n = {}_o\theta_3^n = 0, \quad {}_o\theta_2^n = 2\pi/150. \tag{4.2}$$

Of course, in its common form (called B-DNA) a DNA molecule has a helical repeat length close to 10 base pairs or, equivalently, values of ${}_o\theta_3^n$ close to $\pi/5$, i.e., 36° . In the present case in which the molecule is transversely isotropic in the sense that (4.1) is assumed to hold, one can assign to the numbers ${}_o\theta_i^n$ values that yield a molecule with ${}_o\theta_3^n \equiv \pi/5$ that has the same axial curve when stress-free and a mechanical behavior identical to that of the molecule under consideration. This can be done by putting,⁸ for each subsegment with 10 base-pair steps, in addition to ${}_o\theta_3^n \equiv \pi/5$,

$${}_o\theta_1^k = \frac{2\pi}{150} \sin\left(\frac{\pi}{5}(k-1) + \frac{\pi}{10}\right), \quad {}_o\theta_2^k = \frac{2\pi}{150} \cos\left(\frac{\pi}{5}(k-1) + \frac{\pi}{10}\right), \quad (4.3)$$

with, $k = 1, \dots, 10$. (From this point on, unless stated otherwise, angles are expressed in radians.)

The assumption (4.2) gives us an idealized model in which the molecule is homogeneous and planar in its intrinsic configuration. However, in reality ${}_o\theta_3^n$ is not zero. A molecule obeying (4.3) would have ${}_o\theta_3^n \neq 0$ and be planar in its intrinsic configuration, but it would also have ${}_o\theta_1^n$ and ${}_o\theta_2^n$ strongly dependent on n and exhibiting both positive and negative values, which is not likely to occur.⁹ On the other hand, a molecule that has ${}_o\theta_3^n \neq 0$ and, in addition, has ${}_o\theta_1^n, {}_o\theta_2^n, {}_o\theta_3^n$ independent of n cannot have an intrinsic configuration that is even approximately circular. For then, in the intrinsic configuration the two halves of each helical repeat length would be bent in opposite directions. This is the reason why the 150 base pair minicircles treated in reference [1] (and there called “DNA o-rings”) were taken to be composed of 15 repetitions of a 10 base-pair segment in which 5 base-pairs constitute a homogeneous intrinsically straight subsegment and the remaining 5 constitute a homogeneous intrinsically curved subsegment in which the parameters ${}_o\theta_1^n, {}_o\theta_2^n, {}_o\theta_3^n$ are adjusted so that when the 150 base-pair molecule is closed (i.e., has its ends joined so that its axial curve is a closed curve) it is a stress-free ring. To be specific, the DNA o-rings treated in that paper had $({}_o\rho_1^n, {}_o\rho_2^n, {}_o\rho_3^n) = (0, 0, 3.4)$ for all n , but in each 10 base-pair unit, for the first 5 base pair steps,

$$({}_o\theta_1^n, {}_o\theta_2^n, {}_o\theta_3^n) = \left(0, 0, 36 \frac{\pi}{180}\right), \quad (4.4a)$$

and, for the remaining 5,

$$({}_o\theta_1^n, {}_o\theta_2^n, {}_o\theta_3^n) = \left(0, 7.413 \frac{\pi}{180}, 35.568 \frac{\pi}{180}\right). \quad (4.4b)$$

It should be pointed out that DNA o-rings obtained in this way by joining straight segments with curved segments having ${}_o\theta_3^n \neq 0$ and ${}_o\theta_1^n = 0$ are nearly, but not perfectly, planar and have a chiral structure (i.e., have axial curves that differ from their mirror images).¹⁰

The calculations we report in this paper were performed using the assumption (4.2) which here, as we stated above, is equivalent to the assumption (4.3). We have studied also cases in which (4.4a) and (4.4b) hold and found that, when we make the “transverse symmetry assumptions” (1) and (2), the equilibrium configurations we calculate using (4.2) have axial

⁸This conclusion holds when one defines the variables $\theta_1^n, \theta_2^n, \theta_3^n$ in accord with the procedure introduced in [5] and discussed here in the Appendix. Properties of molecules obeying assumptions of the type (4.3) are discussed in reference [16].

⁹Statistical analysis of X-ray structure data [17] indicates that, in general, ${}_o\theta_1$ is approximately zero and ${}_o\theta_2$ is not negative.

¹⁰The writhe W of a closed curve [9–11] is a useful measure of the (total) chirality of the curve. For the axial curve of a 150 base pair minicircle obeying (4.4a), (4.4b), $W=0.078$.

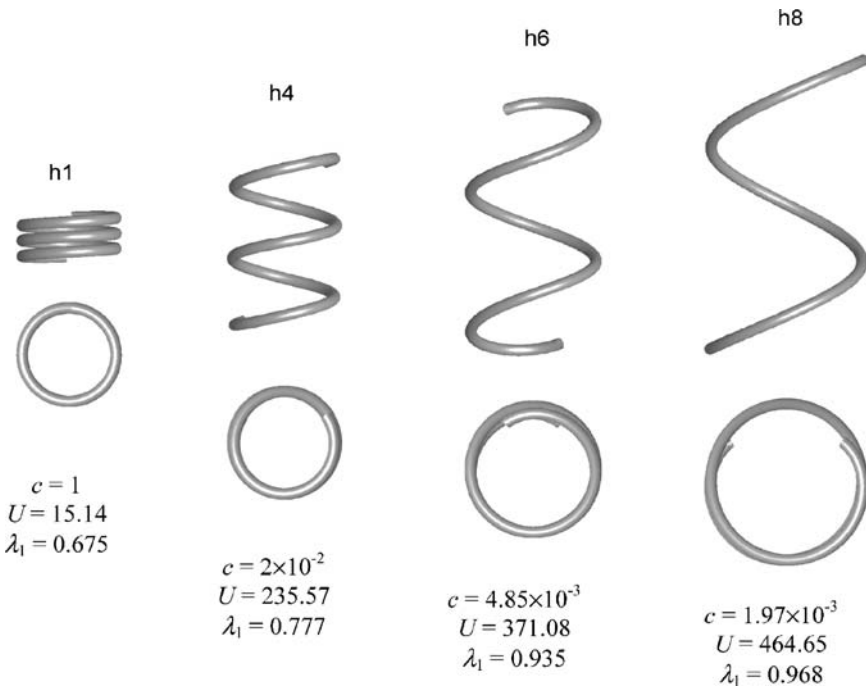


Fig. 3 Four configurations on the primary branch H that are global minimizers of the total energy U at the indicated (monovalent) salt concentration c . The scale of length is the same for each case, and the lines of view for the upper and lower drawings are perpendicular. c is expressed in moles per liter, U in units of kT with $T=300$ K, and, because angles are here expressed in radians, λ_1 , the smallest proper number of the matrix S , is expressed in units of $10^{-2}kT$

curves close to axial curves obtained using (4.4a and 4.4b).¹¹ (The assumption (2) is vital to the validity of this assertion.) Nevertheless, even under the assumptions (1) and (2), the bifurcation diagram implied by (4.2) has a topology that differs from that implied by (4.4a and 4.4b). For a homogeneous molecule obeying (4.2), the system \mathcal{S} is perfect,¹² and, in particular, the branches issuing from an equilibrium configuration $\# \Theta$ that is a bifurcation point can be found using a method in which one starts with a configuration Θ in a neighborhood of $\# \Theta$ and searches for solutions of \mathcal{S} by successive adjustments of trial configurations generated by adding to $\# \Theta$ vectors that are parallel to the characteristic vector for the proper number of $S=[S_{(i,n)(j,m)}]$ that vanishes at $\# \Theta$.¹³ (Here $S_{(i,n)(j,m)}$ is as in equations (3.10) and (3.11)). Both pitchfork and fold bifurcations are observed when (4.2) holds.

For a (periodic but not globally homogeneous) molecule obeying the equations (4.4a and 4.4b), the system \mathcal{S} is imperfect, its equilibrium paths are not connected to each other, and the pitchfork bifurcations of the present system are replaced by folds each of which contains a critical point at which a proper number λ_q of S changes sign and a bifurcation-free equilibrium

¹¹The highly curved sequences found in the kinetoplast DNA of Trypanosomatidae [12–15] more closely resemble a periodic sequence obeying equations (4.4a and 4.4b) than a homogeneous sequence obeying (4.3).

¹²In the sense in which the term is used in [18].

¹³In the present example, the characteristic space of S corresponding to a (vanishing) proper number λ_q is unidimensional. The search procedure just described can be generalized to cases in which proper numbers are degenerate.

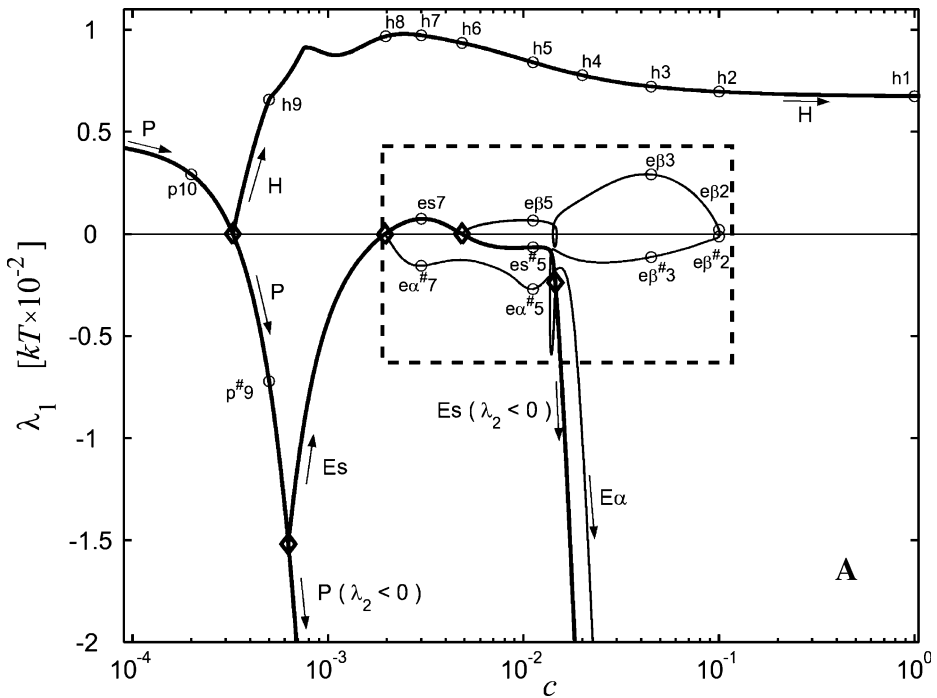


Fig. 4A Bifurcation diagram for equilibrium configurations presented as a graph of λ_1 , the smallest proper number of the matrix S of equation (3.11), versus the salt concentration c . Configurations with $\lambda_1 > 0$ are (locally) stable. Small circles denote configurations shown in Fig. 3 or Figs. 5, 6, 7, 8, 9 and 10. The (diamond) indicates a bifurcation point. The stem branch P and the primary branches H and Es are drawn in boldface, the secondary branches $E\alpha$ and $E\beta$ in lightface

path is nearby. (Analogues in the theory of elasticity are discussed in the text of Thompson and Hunt [18].) The observed behavior of the imperfect system obeying (4.4a and 4.4b) is the result of (a) non-planarity and chirality of the axial curve in the stress-free configuration and (b) the fact that a DNA molecule containing an integral number of helical repeat units obeying (4.4a and 4.4b) has intrinsic directionality, because the 5 base-pair segment at one of its ends is intrinsically straight while that at the other end is intrinsically curved. In a paper now in preparation we shall present detailed calculations illustrating the similarities and differences between the behavior of a perfect system S_p that obeys (4.2) and an imperfect system S_i of the same order ($3N$) that obeys the more realistic assumption (4.4a and 4.4b).

A DNA molecule is approximately a tube with a cross sectional diameter of 20 Å and is so represented in Fig. 3 and Figs. 5, 6, 7, 8, 9 and 10. In its intrinsic configuration, the 450 base pair DNA molecule under consideration would have an axial curve with the form of a triply wound (planar) circle. Because the molecule cannot penetrate itself, that stress-free configuration is not physically attainable. For values of c less than 1.2 M (1.2 molar) our calculations showed the existence of stable equilibrium configurations for which the axial curve of the molecule is close to a helix with a pitch greater than 20 Å, and such configurations, as they are free from self-penetration, are physically attainable. The examples in Fig. 3, for values of c in a range of interest to experimenters,¹⁴ lie on the branch labeled H in the bifurcation diagram of Fig. 4. Each point on that branch

¹⁴DNA denatures when c is less than 10^{-3} M.

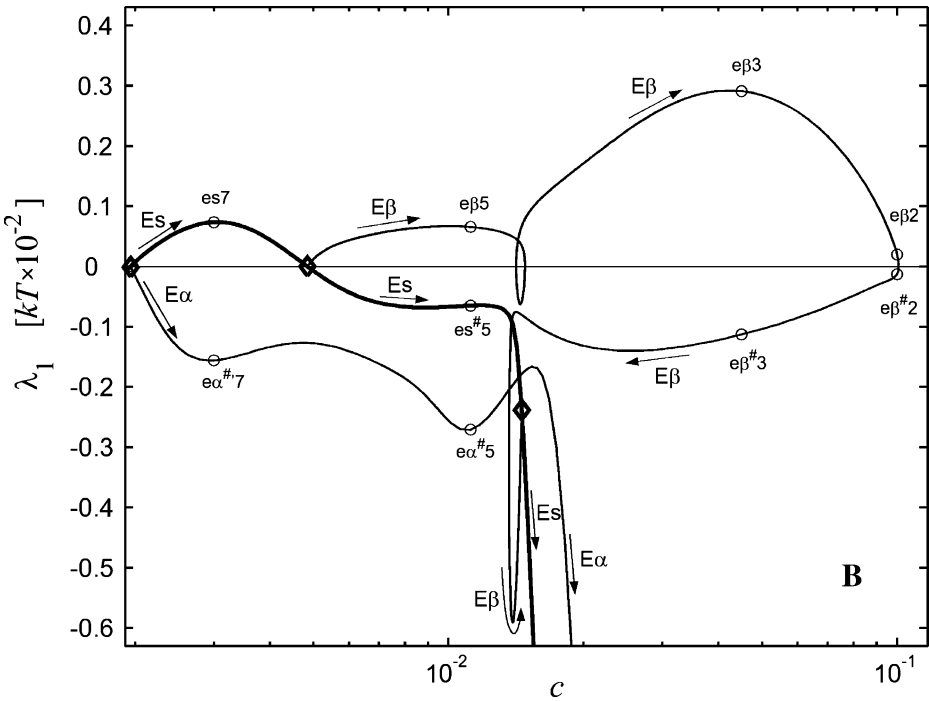


Fig. 4B Enlargement of the rectangular region that is bounded by dashed lines in Fig. 4A

corresponds to two solutions of (2.28) of equal energy but opposite chirality (the approximating helix is right-handed for one and left-handed for the other, but in the present case are otherwise congruent). As branch H lies in a region where λ_1 is positive, each configuration on it is stable. Our careful and extensive calculations indicate that a much stronger statement can be made: each configuration on branch H is not just a local but also a global minimizer of the total energy U for the same value of c .

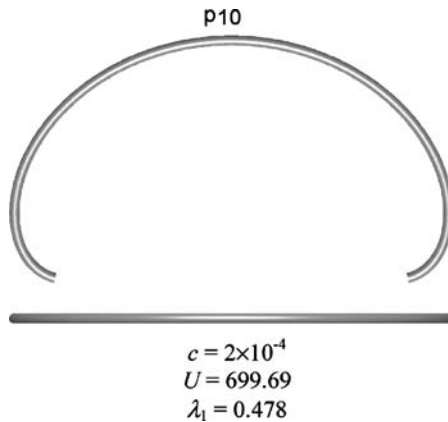


Fig. 5 The planar configuration on the stem branch P with $c = 2 \times 10^{-4}$ M. This configuration is globally stable

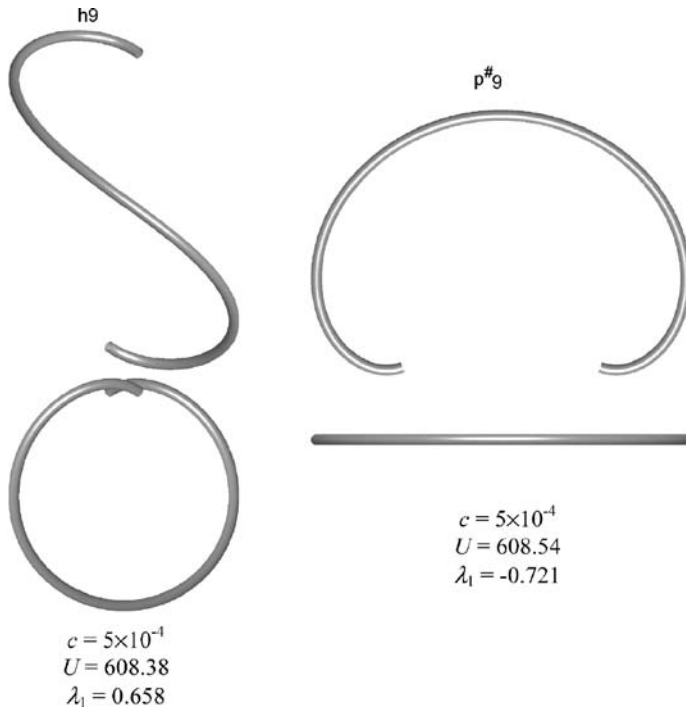


Fig. 6 Two equilibrium configurations with $c = 5 \times 10^{-4}$ M. The planar configuration p#9 is unstable. (The sharp symbol indicates lack of stability.) The configuration h9 is globally stable

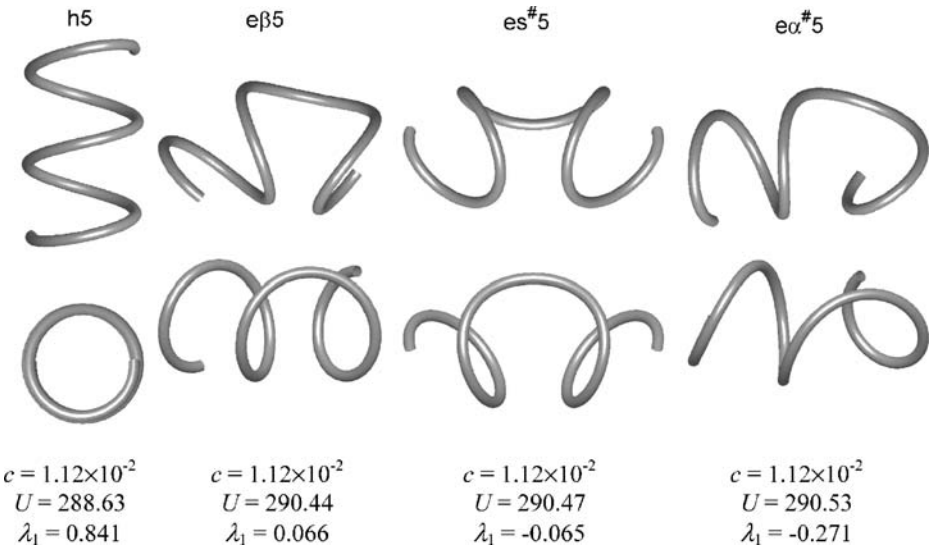


Fig. 7 Four distinct equilibrium configurations with $c = 1.12 \times 10^{-2}$ M. The configurations es#5 and eα#5 are unstable; eβ5 is locally stable; h5 is globally stable

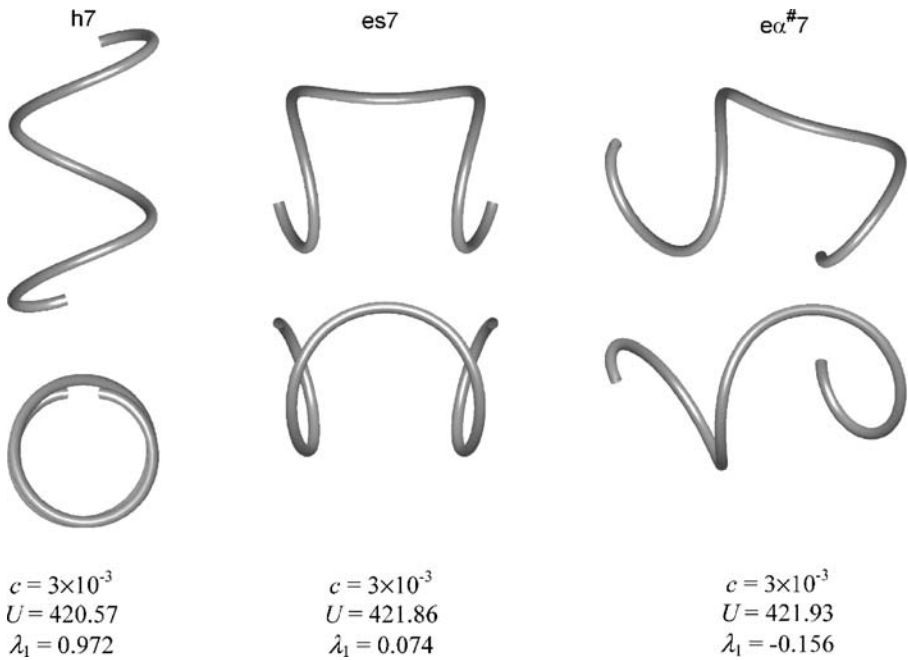


Fig. 8 Three distinct equilibrium configurations with $c = 3 \times 10^{-3}$ M. The configuration eα[#]7 is unstable; es7 is locally stable; h7 is globally stable

Branch H originates at a pitch fork bifurcation of a branch labeled P, each point of which corresponds to a single planar equilibrium configuration. At this bifurcation point $c = c^* = 3.26 \times 10^{-4}$ M and $\lambda_1 = 0$. For $c > c^*$ each configuration in P is unstable; for $c < c^*$ the configurations in P are global minimizers of U . A stable configuration that lies on P where $c = 2 \times 10^{-4}$ M is shown in Fig. 5. That configuration and the helical configurations

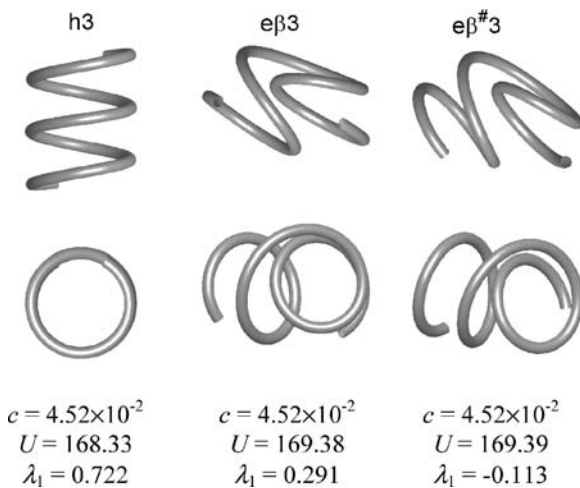


Fig. 9 Three distinct equilibrium configurations with $c = 4.52 \times 10^{-2}$ M. The configuration eβ[#]3 is unstable; eβ3 is locally stable; h3 is globally stable

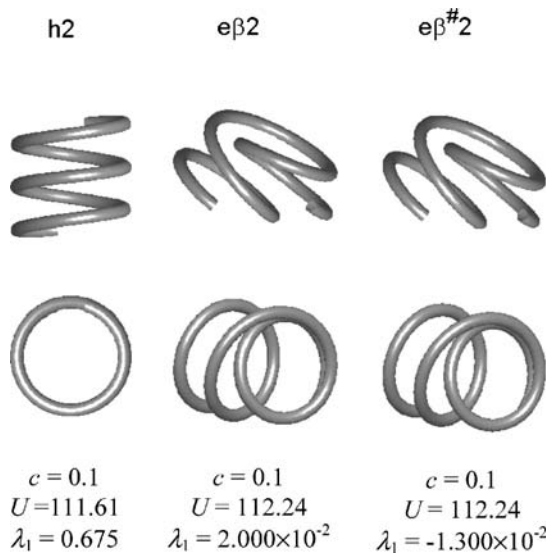


Fig. 10 Three distinct equilibrium configurations with $c=0.1$ M, a value of c less than but very close to the critical value $c^{\#}=0.101$ M. The configuration $e\beta^{\#}2$ is unstable; $e\beta 2$ is locally stable; $h2$ is globally stable

shown in Fig. 3 illustrate the sensitivity of globally stable equilibrium configurations to changes in salt concentration. In Fig. 6 one sees two equilibrium configurations at a value of c close to but above c^* , the configuration $h9$ is in H and the other, $p^{\#}9$, is in P. The configuration $h9$ is chiral and globally stable but is not very well approximated by a helix.

The branch P may be considered a *stem branch* containing bifurcation points at which primary branches originate. As one moves along P in the direction of increasing c , one encounters first the branch H and then a branch labeled Es that originates at a pitchfork bifurcation at which $\lambda_2=0$ and $c = 6.30 \times 10^{-4}$ M. The configurations on branch Es are symmetric in the sense that their axial curves have a plane of symmetry. In the classical theory of intrinsically helical rods, configurations that have been subjected to tensile loads and have, like those on branch Es, two approximately helical subregions of opposite handedness and a separating transition region (see, e.g., the unstable configuration $es^{\#}5$ in Fig. 7, and the locally stable configuration $es7$ in Fig. 8) are occasionally called “perversions”.¹⁵ We here prefer to say that the configurations $es^{\#}5$ and $es7$ are “everted helical configurations”.

Secondary branches labeled $E\alpha$ and $E\beta$ originate at bifurcation points of the primary branch Es with $\lambda_1=0$ and are comprised of configurations that are not symmetric. Two

¹⁵Domokos and Healey [19], in a recent study of the theory of transversely isotropic, inextensible Kirchhoff rods of finite length with uniform nonzero intrinsic curvature and zero intrinsic torsion, developed a theory appropriate to cases in which such a rod is subject to the following end conditions: the two ends are clamped so that their cross sections stay perpendicular to the line ℓ connecting their mid-points, neither end is permitted to rotate about ℓ , and the applied tensile force f acts along ℓ . They find that, when the rod’s intrinsic curvature and the (positive) tension f are in appropriate ranges, the rod has stable configurations, called “perversions”, that are strikingly similar to the “everted helical configurations” found in our investigation. (In an earlier investigation, Goriely and Tabor [20] found, in the context of periodic configurations for infinite rods, equilibrium solutions of the type just described for finite rods subject to end conditions.) We believe it interesting that these two types of results, with one obtained for curved rods free of long range forces but subject to tensile loads at their ends, and the other for curved rodlike structures that have free ends but bear internal electrostatic forces of repulsion, give rise to such closely similar configurations, although in one case the ends are free of applied forces and moments and in the other are clamped in such way that, at each end of a rod, the tangent to the rod axis is parallel to ℓ .

examples, $\epsilon\alpha^{\#5}$ and $\epsilon\beta 5$, are shown in Fig. 7. (See also $\epsilon\alpha^{\#7}$ in Fig. 8, $\epsilon\beta^{\#3}$, $\epsilon\beta 3$ in Fig. 9, and $\epsilon\beta^{\#2}$, $\epsilon\beta 2$ in Fig. 10.) The bifurcation diagram for the DNA molecule under consideration has regions in which several distinct equilibrium configurations with more than one of them stable occur at a single value of c . This is the case for c in the range of values appropriate to Fig. 4a.¹⁶ Shown in Figs. 7, 8, and 9 are 4 equilibrium configurations that occur at $c = 1.12 \times 10^{-2}$ M, 3 at $c = 3 \times 10^{-3}$ M, and 3 at $c = 4.52 \times 10^{-2}$ M; in each of these cases two of the distinct configurations are stable.¹⁷ In the small subrange $1.41 \times 10^{-2} \text{M} < c < 1.48 \times 10^{-2} \text{M}$ of the range shown in Fig. 4b, i.e., for values of c between the first and second depicted folds on the branch $E\beta$, there are 3 distinct stable configurations, with 2 on the branch $E\beta$ and 1 on the branch H. For values of c greater than $c^{\#} = 0.101$ M (a critical value attained at the point on the third fold of the branch $E\beta$ at which $\lambda_1 = 0$), configurations in the branch H are the only stable configurations. Therefore a small increase in c from a value below $c^{\#}$ to a value above $c^{\#}$ will give rise to a transition from a locally stable configuration on the branch $E\beta$ to a globally stable configuration on the branch H.¹⁸ In Fig. 10 are shown 2 configurations on the branch $E\beta$ and a configuration on the branch H for $c = 0.1$ M, a value that is very close to, but less than, $c^{\#}$.

Acknowledgements We thank Professor Gabor Domokos for useful discussions about the stability of computational schemes for solving non-linear systems of equations related to those considered here. This research was supported by the National Science Foundation under Grants DMS-0514470 and DMS-0516646.

Appendix

In this appendix we first discuss El Hassan and Calladine’s procedure [5] for constructing their relation between the six kinematical variables $\theta_1^n, \theta_2^n, \theta_3^n, \rho_1^n, \rho_2^n, \rho_3^n$ and the numbers $D_{ij}^n = \mathbf{d}_i^n \cdot \mathbf{d}_j^{n+1}$ and $r_i^n = \mathbf{r}^n \cdot \mathbf{d}_i^n$; we then give a derivation of the expression presented in reference [1] for the quantities $\Gamma_{ij}^n = \widehat{\Gamma}_{ij}(\theta_1^n, \theta_2^n, \theta_3^n)$ appearing here in equations (2.11), (2.14), and (3.13).

Let $\mathbf{d}_1^n, \mathbf{d}_2^n, \mathbf{d}_3^n$ and $\theta_1^n, \theta_2^n, \theta_3^n$ be given, and let the angles ξ^n and ϕ^n and a unit vector \mathbf{d}_ϕ^n (called the “hinge vector”), in the plane of \mathbf{d}_1^n and \mathbf{d}_2^n , be defined by the relations:

$$\xi^n = \sqrt{(\theta_1^n)^2 + (\theta_2^n)^2}, \quad \theta_1^n = \xi^n \sin(\phi^n), \quad \theta_2^n = \xi^n \cos(\phi^n), \tag{A.1}$$

$$\mathbf{d}_\phi^n = -\mathbf{d}_1^n \sin\left(\frac{\theta_3^n}{2} - \phi^n\right) + \mathbf{d}_2^n \cos\left(\frac{\theta_3^n}{2} - \phi^n\right). \tag{A.2}$$

¹⁶For each value of c for which there are stable and/or unstable configurations on branches seen in Fig. 4b, there is also a (stable) configuration that is on the branch H seen not in Fig. 4b but in Fig. 4a.

¹⁷With the branch P a singular exception, the branches seen in Fig. 4 are generally sets of several branches that can be mapped into each other by energy preserving transformations of their constituent configurations. These transformations include that for which $(\Delta\theta_1^n, \Delta\theta_2^n, \Delta\theta_3^n) \mapsto (-\Delta\theta_1^n, \Delta\theta_2^n, -\Delta\theta_3^n)$ for each n (and hence that changes only the chirality or “handedness” of the configuration) and that for which $(\Delta\theta_1^n, \Delta\theta_2^n, \Delta\theta_3^n) \mapsto (-\Delta\theta_1^{N-n+1}, \Delta\theta_2^{N-n+1}, \Delta\theta_3^{N-n+1})$ for each n . In this paper when counting configurations we consider two configurations the same if they are related by energy preserving transformations of these types. For configurations on branches of order higher than 2 (which are not discussed in this paper), symmetry groups characterized by energy preserving transformations other than those generated by the two just described are relevant.

¹⁸This critical value $c^{\#}$ corresponds to an ionic strength not far from that occurring under physiological conditions.

By applying to $\mathbf{d}_1^n, \mathbf{d}_2^n, \mathbf{d}_3^n$ a positive rotation about \mathbf{d}_ϕ^n of magnitude $\xi^n/2$ one obtains an orthonormal triad $\mathbf{d}_1^{n+\alpha}, \mathbf{d}_2^{n+\alpha}, \mathbf{d}_3^{n+\alpha}$ which one then rotates about $\mathbf{d}_3^{n+\alpha}$ through the angle $\theta_3^n/2$ to obtain another orthonormal triad, $\mathbf{d}_1^{n+\frac{1}{2}}, \mathbf{d}_2^{n+\frac{1}{2}}, \mathbf{d}_3^{n+\frac{1}{2}}$, which in reference [5] is called the “mid-step triad.” (Of course, $\mathbf{d}_3^{n+\frac{1}{2}} = \mathbf{d}_3^{n+\alpha}$). Here, as in [5], the displacement variables $\rho_1^n, \rho_2^n, \rho_3^n$ are, by definition, the components of \mathbf{r}^n with respect to the elements of the mid-step triad:

$$\rho_i^n = \mathbf{r}^n \cdot \mathbf{d}_i^{n+\frac{1}{2}}. \tag{A.3}$$

This last equation can be written in the form (2.3) with the numbers R_{ij}^n the components of the vectors $\mathbf{d}_1^{n+\frac{1}{2}}, \mathbf{d}_2^{n+\frac{1}{2}}, \mathbf{d}_3^{n+\frac{1}{2}}$ with respect to the basis $\mathbf{d}_1^n, \mathbf{d}_2^n, \mathbf{d}_3^n$:

$$R_{ij}^n = \mathbf{d}_i^n \cdot \mathbf{d}_j^{n+\frac{1}{2}}. \tag{A.4}$$

The procedure just described yields an explicit expression [5] for the function \widehat{R}_{ij} in (2.3), namely,

$$R_{ij}^n = \widehat{R}_{ij}(\theta_1^n, \theta_2^n, \theta_3^n) = \sum_{k=1}^3 \sum_{l=1}^3 Z_{ik} \left(\frac{\theta_3^n}{2} - \phi^n \right) Y_{kl} \left(\frac{\xi^n}{2} \right) Z_{lj}(\phi^n), \tag{A.5}$$

where $Y_{ij}(\zeta)$ and $Z_{ij}(\zeta)$ are, for each ζ , elements of the following rotation matrices:

$$[Y_{ij}(\zeta)] = \begin{bmatrix} \cos(\zeta) & 0 & \sin(\zeta) \\ 0 & 1 & 0 \\ -\sin(\zeta) & 0 & \cos(\zeta) \end{bmatrix}, \quad [Z_{ij}(\zeta)] = \begin{bmatrix} \cos(\zeta) & -\sin(\zeta) & 0 \\ \sin(\zeta) & \cos(\zeta) & 0 \\ 0 & 0 & 1 \end{bmatrix}. \tag{A.6}$$

The (fixed in space) hinge vector \mathbf{d}_ϕ^n in equations (A.2) can be expressed in terms of its components with respect to the mid-step triad as

$$\mathbf{d}_\phi^n = \mathbf{d}_1^{n+\frac{1}{2}} \sin(\phi^n) + \mathbf{d}_2^{n+\frac{1}{2}} \cos(\phi^n). \tag{A.7}$$

The triad $\mathbf{d}_1^{n+1}, \mathbf{d}_2^{n+1}, \mathbf{d}_3^{n+1}$ can be obtained by applying to $\mathbf{d}_1^{n+\frac{1}{2}}, \mathbf{d}_2^{n+\frac{1}{2}}, \mathbf{d}_3^{n+\frac{1}{2}}$ first a rotation through an angle $\theta_3^n/2$ about $\mathbf{d}_3^{n+\frac{1}{2}}$ and then a rotation of magnitude $\xi^n/2$ about the hinge vector \mathbf{d}_ϕ^n . As the second rotation brings the original triad $\mathbf{d}_1^{n+\frac{1}{2}}, \mathbf{d}_2^{n+\frac{1}{2}}, \mathbf{d}_3^{n+\frac{1}{2}}$ into coincidence with $\mathbf{d}_1^{n+1}, \mathbf{d}_2^{n+1}, \mathbf{d}_3^{n+1}$, for the components of \mathbf{d}_j^{n+1} with respect to $\mathbf{d}_i^{n+\frac{1}{2}}$ we have

$$\mathbf{d}_i^{n+\frac{1}{2}} \cdot \mathbf{d}_j^{n+1} = \sum_{k=1}^3 \sum_{l=1}^3 Z_{ik}(-\phi^n) Y_{kl} \left(\frac{\xi^n}{2} \right) Z_{lj} \left(\frac{\theta_3^n}{2} + \phi^n \right), \tag{A.8}$$

and as

$$D_{ij}^n = \mathbf{d}_i^n \cdot \mathbf{d}_j^{n+1} = \sum_{k=1}^3 \left(\mathbf{d}_i^n \cdot \mathbf{d}_k^{n+\frac{1}{2}} \right) \left(\mathbf{d}_k^{n+\frac{1}{2}} \cdot \mathbf{d}_j^{n+1} \right), \tag{A.9}$$

in view of (A.4) and (A.8) we have [5],

$$D_{ij}^n = \widehat{D}_{ij}(\theta_1^n, \theta_2^n, \theta_3^n) = \sum_{k=1}^3 \sum_{l=1}^3 Z_{ik} \left(\frac{\theta_3^n}{2} - \phi^n \right) Y_{kl}(\xi^n) Z_{lj} \left(\frac{\theta_3^n}{2} + \phi^n \right). \tag{A.10}$$

If we follow an argument given in [1] and note that each variation in the orthonormal triad $\mathbf{d}_1^n, \mathbf{d}_2^n, \mathbf{d}_3^n$ is determined by a vector $\boldsymbol{\gamma}^n$ as shown in equations (3.5), i.e., $\delta \mathbf{d}_i^n = \boldsymbol{\gamma}^n \times \mathbf{d}_i^n$, the relations $D_{ij}^n = \mathbf{d}_i^n \cdot \mathbf{d}_j^{n+1}$ will yield

$$\sum_{j=1}^3 \sum_{l=1}^3 D_{kj}^n \frac{\partial \widehat{D}_{ij}}{\partial \theta_l^n} \delta \theta_l^n = \sum_{j=1}^3 e_{kij} \mathbf{d}_j^n \cdot (\boldsymbol{\gamma}^{n+1} - \boldsymbol{\gamma}^n), \tag{A.11}$$

and if we make use of the fact that the matrices $\sum_{j=1}^3 D_{kj}^n \frac{\partial \widehat{D}_{ij}}{\partial \theta_l^n}$ are skew, i.e., that

$$\sum_{j=1}^3 D_{kj}^n \frac{\partial \widehat{D}_{ij}}{\partial \theta_l^n} = - \sum_{j=1}^3 D_{ij}^n \frac{\partial \widehat{D}_{kj}}{\partial \theta_l^n}, \quad l = 1, 2, 3, \tag{A.12}$$

we can write (A.11) in the form

$$\sum_{l=1}^3 \Xi_{il}^n \delta \theta_l^n = \mathbf{d}_i^n \cdot (\boldsymbol{\gamma}^{n+1} - \boldsymbol{\gamma}^n), \tag{A.13}$$

where the components of the matrix $[\Xi_{il}^n]$ are

$$\Xi_{1l}^n = \sum_{j=1}^3 D_{2j}^n \frac{\partial \widehat{D}_{3j}}{\partial \theta_l^n}, \quad \Xi_{2l}^n = \sum_{j=1}^3 D_{3j}^n \frac{\partial \widehat{D}_{1j}}{\partial \theta_l^n}, \quad \Xi_{3l}^n = \sum_{j=1}^3 D_{1j}^n \frac{\partial \widehat{D}_{2j}}{\partial \theta_l^n}. \tag{A.14}$$

As was observed in [1] in a more general context, throughout the range of values of $\theta_1^n, \theta_2^n, \theta_3^n$ appropriate to a DNA molecule, the matrix $[\Xi_{il}^n]$ with components $\Xi_{il}^n = \widehat{\Xi}_{il}(\theta_1^n, \theta_2^n, \theta_3^n)$ is an invertible matrix with inverse $[\Xi_{il}^n]^{-1}$, and hence one can solve equation (A.13) for $\delta \theta_l^n$ to obtain the relation (3.4) in which the numbers $\Gamma_{il}^n = \Gamma_{il}(\theta_1^n, \theta_2^n, \theta_3^n)$ are the components of the transpose of $[\Xi_{il}^n]^{-1}$. It follows from the equations (A.6), (A.10), and (A.14) that

$$\Gamma_{ij}^n = \begin{bmatrix} -\frac{\theta_1^n}{\xi^n} s^n + \frac{\theta_2^n t^n}{2 \tan(\xi^n/2)} & -\frac{\theta_2^n}{\xi^n} s^n - \frac{\theta_1^n t^n}{2 \tan(\xi^n/2)} & \tan(\xi^n/2) t^n \\ \frac{\theta_1^n t^n}{\xi^n} + \frac{\theta_2^n s^n}{2 \tan(\xi^n/2)} & \frac{\theta_2^n t^n}{\xi^n} - \frac{\theta_1^n s^n}{2 \tan(\xi^n/2)} & \tan(\xi^n/2) s^n \\ -\theta_2^n/2 & \theta_1^n/2 & 1 \end{bmatrix}, \tag{A.15}$$

where

$$t^n = \cos\left(\frac{\theta_3^n}{2} - \phi^n\right), \quad s^n = \sin\left(\frac{\theta_3^n}{2} - \phi^n\right). \tag{A.16}$$

The present equation (A.15) is the same as equation (A.1) of [1].

References

1. Coleman, B.D., Olson, W.K., Swigon, D.: Theory of sequence-dependent DNA elasticity. *J. Chem. Phys.* **118**, 7127–7140 (2003)
2. Olson, W.K., Swigon, D., Coleman, B.D.: Implications of the dependence of the elastic properties of DNA on nucleotide sequence. *Philos. Trans. R. Soc. Lond. A* **362**, 1403–1422 (2004)
3. Olson, W.K., Bansal, M., Burley, S.K., Dickerson, R.E., Gerstein, M., Harvey, S.C., Heinemann, U., Lu, X., Neidle, S., Shakked, Z., Wolberger, C., Berman, H.M.: A standard reference frame for the description of nucleic acid base-pair geometry. *J. Mol. Biol.* **313**, 229–237 (2001)

4. Zhurkin, V.B., Lysov, Y.P., Ivanov, V.: Anisotropic flexibility of DNA and the nucleosomal structure. *Nucleic Acids Res.* **6**, 1081–1096 (1979)
5. El Hassan, M.A., Calladine, C.R.: The assessment of the geometry of dinucleotide steps in double-helical DNA: A new local calculation scheme. *J. Mol. Biol.* **251**, 648–664 (1995)
6. Manning, G.S.: Limiting laws and counterion condensation in polyelectrolyte solutions: I. Colligative properties. *J. Chem. Phys.* **51**, 924–933 (1969)
7. Westcott, T.P., Tobias, I., Olson, W.K.: Modeling self-contact forces in the elastic theory of DNA supercoiling. *J. Chem. Phys.* **107**, 3967–3980 (1997)
8. Fenley, M.O., Manning, G.S., Olson, W.K.: Approach to the limit of counterion condensation. *Biopolymers* **30**, 1191–1203 (1990)
9. White, J.H.: Self-linking and the Gauss integral in higher dimensions. *Am. J. Math.* **91**, 693–728 (1969)
10. Fuller, F.B.: The writhing number of a space curve. *Proc. Natl. Acad. Sci. U. S. A.* **68**, 815–819 (1971)
11. White, J.H.: *Mathematical Methods for DNA Sequences*. CRC, Boca Raton, Florida (1989)
12. Marini, J.C., Levene, S.D., Crothers, D.M., Englund, P.T.: Bent helical structure in kinetoplast DNA. *Proc. Natl. Acad. Sci. USA* **79**, 7664–7668 (1982) (Correction *ibid.* **80**, 7678 (1983))
13. Diekmann, S., Wang, J.C.: On the sequence determinants and exibility of the kinetoplast DNA fragment with abnormal gel electrophoretic mobilities. *J. Mol. Biol.* **186**, 1–11 (1985)
14. Haran, T.E., Kahn, J.D., Crothers, D.M.: Sequence elements responsible for DNA curvature. *J. Mol. Biol.* **244**, 135–144 (1994)
15. Griffith, J., Bleyman, M., Rauch, C.A., Kitchin, P.A., Englund, P.T.: Visualization of the bent helix in kinetoplast DNA by electron microscopy. *Cell* **46**, 717–724 (1986)
16. Calladine, C.R., Drew, H.R., Luisi, B.F., Travers, A.A.: *Understanding DNA*, 3rd edn. Elsevier, London (2004)
17. Olson, W.K., Gorin, A.A., Lu, X.-J., Hock, L.M., Zhurkin, V.B.: DNA sequence-dependent deformability deduced from protein-DNA crystal complexes. *Proc. Natl. Acad. Sci. U. S. A.* **95**, 11163–11168 (1998)
18. Thompson, J.M.T., Hunt, G.W.: *A General Theory of Elastic Stability*. Wiley, London (1973)
19. Domokos, G., Healey, T.J.: Multiple helical perversions of finite intrinsically curved rods. *Int. J. Bifurc. Chaos* **15**, 871–890 (2005)
20. Goriely, A., Tabor, M.: The mechanics and dynamics of tendril perversion in climbing plants. *Phys. Lett. A.* **250**, 311–318 (1998)